Effect of the Epoxy Resin Chemistry on the Viscoelasticity of Its Cured Product

J. S. Nakka,[1] K. M. B. Jansen,[1] L. J. Ernst,[1] W. F. Jager[2]

[1]*Delft University of Technology, Mekelweg 2, 2628 CD Delft, The Netherlands*
[2]*Delft University of Technology, Julianalaan 136, 2628 BL Delft, The Netherlands*

Received 27 July 2007; accepted 3 November 2007
DOI 10.1002/app.27740
Published online 23 January 2008 in Wiley InterScience (www.interscience.wiley.com).

ABSTRACT: A detailed study investigating the relation between the initial resin composition and mixing ratio on the viscoelastic behavior was performed. The resin system, containing a difunctional aromatic epoxy (DER 332), was mixed with three aliphatic amines containing functionalities of 2, 3, and 4 in different stoichiometric mixing ratios and was cured. For each of the cured mixtures, the viscoelastic master curve and corresponding shift factors were determined. Depending on the crosslink density, the viscoelastic curves shifted by about 12 decades with respect to the frequency scale. This shift in the viscoelastic curve was predicted by the combination of the Miller–Macosko theory for crosslink density with a parameterized Havriliak–Negami model for the master curve. A single set of 9 parameters turned out to be sufficient to describe all viscoelastic data. © 2008 Wiley Periodicals, Inc. J Appl Polym Sci 108: 1414–1420, 2008

Key words: crosslinking; glass transition; resin; thermosets; viscoelastic properties

INTRODUCTION

The reliability of any product depends on its long-term performance. The end-product performance of thermoset materials depends mainly on the viscoelasticity. The position of the viscoelastic-transition region is characteristic for the determination of the thermomechanical properties of these thermoset materials. This viscoelastic-transition region of the thermosetting materials is sensitive to the variation of the reacting mixture (or group) functionality, mixing ratio, conversion, and curing conditions.[1] To predict the effect of such changes, a model is proposed that relates the chemistry of the reacting resin–hardener mixtures to the final viscoelastic behavior. The proposed model can be achieved in two steps.

First, we assume that the governing factor for predicting the viscoelastic properties of thermosets is the crosslink density. Because the crosslink density is a function of the reacting functional groups, mixing ratio, and conversion, these inputs have to be determined. Theoretically, the crosslink density can be predicted by the Macosko–Miller theory,[2,3] and experimentally, it can be estimated from the rubbery modulus (E_r) with the concept of rubber elasticity. In the second step, we use the thus calculated crosslink density (ν_c^{calc}) for the shape of the viscoelastic master curve. In this work, the effect of the epoxy/amine functionality, mixing ratio, and conversion on the viscoelastic behavior is discussed. Stoichiometric ratios of an epoxy to an amine with various functionalities were cured so that full conversion of the epoxy was achieved. The fully cured products were then tested for their thermomechanical properties in the tension mode in a dynamic mechanical analyzer. Time–temperature superposition was applied to the data obtained from the dynamic mechanical analysis (DMA) tests. We then parameterized the shape changes of the relaxation master curves. This resulted in a set of parameters including the glassy modulus (E_g), E_r, the position of the glass-transition region (relaxation time constant), and the shape of the glass-transition region. The obtained parameters were then related to the crosslink density. The Havriliak–Negami fitting function was used to describe the viscoelastic behavior of these resin systems.

It is clear that this way of predicting the viscoelastic behavior from the knowledge of the constituent properties can never be universally valid, but the idea is that it will be applicable to describe the effect of the formulation for a set of closely related monomer molecules, such as monomers that differ in only functionality (number of reactive groups). Therefore, if this is understood, the initial resin chemistry can be tailored to meet the desired viscoelasticity, which can very well be used for the end applications.

EXPERIMENTAL

Materials

Bisphenol A diglycidyl ether (DER 332; 97%) and three aliphatic amine curing agents—ethylenediamine

Correspondence to: J. S. Nakka (n.j.suman@3me.tudelft.nl).

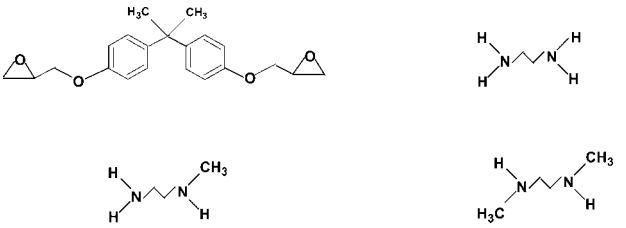

Figure 1 Compound names, structures, and average functionality (f) values of the epoxy and three aliphatic amines: (a) DER 332 (f = 2), (b) EDA (f = 4), (c) MEDA (f = 3), and (d) DMEDA (f = 2).

(EDA; 99% pure), methyl ethylenediamine (MEDA; 95% pure), dimethyl ethylenediamine (DMEDA; 99% pure)—were purchased from Sigma–Aldrich Logistik GmbH (Schnelldorf, Germany). These materials were not purified and were used as received. The purities of the amines were checked with gas chromatography/mass spectroscopy. The chemical structures of the epoxy and amines are shown in Figure 1, and the curing reaction between them is shown in Figure 2.

Calculation of the average functionality and stoichiometric ratio

Let us consider an arbitrary mixture of polydisperse monomers with f_i functional groups (A_i) and monomers with g_j functional groups (B_j). The number-average functionalities then become

$$\bar{f}_{n,A} = \frac{\sum n_{Ai0} f_i}{\sum n_{Ai0}}, \quad \bar{g}_{n,B} = \frac{\sum n_{Bj0} g_j}{\sum n_{Bj0}} \tag{1}$$

where n_{Ai0} and n_{Bj0} denote the initial number of moles of the A_i and B_j monomers, respectively. For future use, we also define the molar fractions of crosslinkable A and B groups (a_i and b_j, respectively) as follows:

$$a_i = \frac{n_{Ai0} f_i}{\sum n_{Ai0} f_i}, \quad b_j = \frac{n_{Bj0} g_j}{\sum n_{Bj0} g_j} \tag{2}$$

The stoichiometric ratio is defined as the initial ratio of all available A groups to all B groups (r_A):

$$r_A = \frac{\text{Initial number of A groups}}{\text{Initial number of B groups}} = \frac{\sum n_{Ai0} f_i}{\sum n_{Bj0} g_j} \tag{3}$$

For equal numbers of A and B groups, this ratio equals unity. Consider now the case in which there are more B groups available ($r_A < 1$) and the A groups have reacted to the extent of p_A (which is defined as the number of reacted A groups divided by the initial number of A groups). Because the number of reacted B groups equals that of the

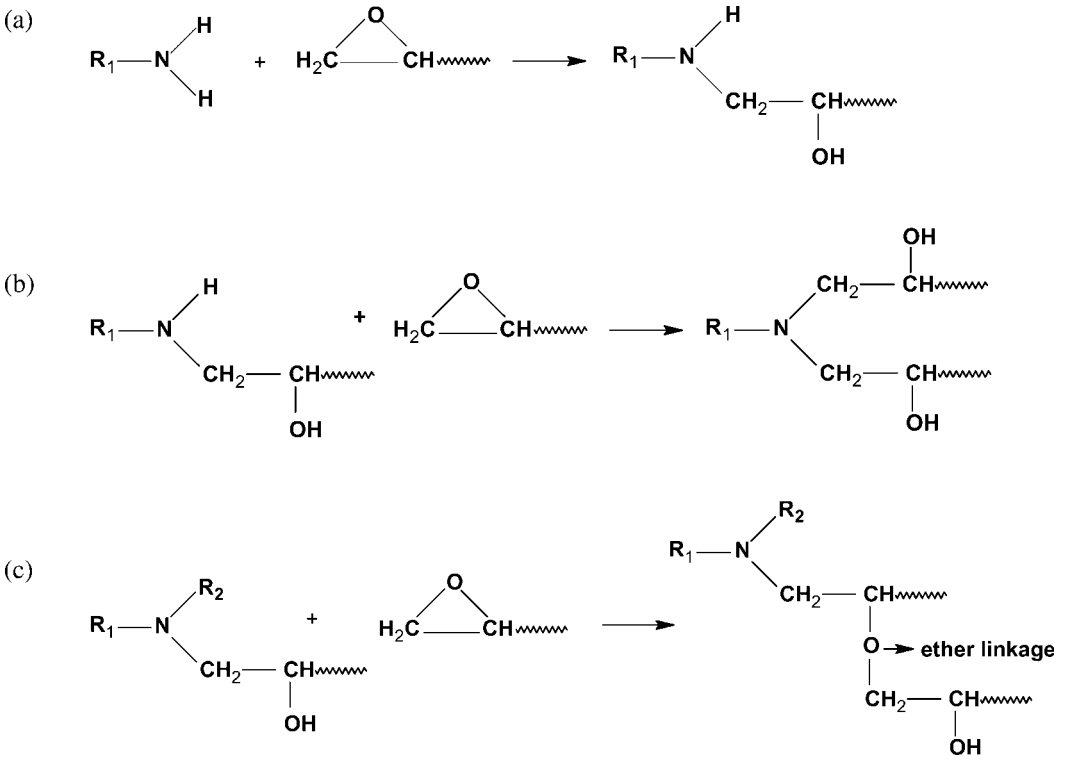

Figure 2 (a) Epoxide ring-opening reaction with the primary amine, (b) epoxide ring-opening reaction with the secondary amine, and (c) etherification reaction between the hydroxyl group of the reacted epoxy and unreacted epoxy groups (usually at temperatures above 100°C) or homopolymerization of the epoxy.

TABLE I
Average Functionality (f) Values, Compositions, and Postcure Schedules of Different Stoichiometric Mixing Ratios

f	Sample	Stoichiometric mixing ratio	Postcure
2.0	DD_1_1	1 DER332 + 1 DMEDA	4 h at 100°C
2.2	DMD_1_03_07	1 DER332 + 0.3 MEDA + 0.7 DMEDA	4 h at 100°C
2.4	DMD_1_05_05	1 DER332 + 0.5 MEDA + 0.5 DMEDA	4 h at 100°C
2.6	DMD_1_07_03	1 DER332 + 0.7 MEDA + 0.3 DMEDA	4 h at 100°C
3.0	DM_1_1	1 DER332 + 1 MEDA	4 h at 150°C
3.2	DEM_1_03_07	1 DER332 + 0.3 EDA + 0.7 MEDA	3 h at 150°C
3.4	DEM_1_05_05	1 DER332 + 0.5 EDA + 0.5 MEDA	3 h at 150°C
3.6	DEM_1_07_03	1 DER332 + 0.7 EDA + 0.3 MEDA	3 h at 150°C
4.0	DE_1_1	1 DER332 + 1 EDA	4 h at 150°C

reacted A groups, the conversion of B (p_B) can then be expressed as follows:

$$p_B = \frac{\text{Number of reacted B groups}}{\text{Initial number of B groups}} = \frac{\text{Number of reacted A groups}}{\text{Initial number of B groups}} = p_A r \qquad (4)$$

Neat Resin Castings

Preparation

Neat resin castings for DMA studies were prepared in aluminum molds. The aluminum mold consisted of an aluminum insert with gaps of 6.0 × 1.5 × 3 mm^3 and was fastened between two aluminum plates into which the premixed resin was poured and cured at different curing schedules. A high-temperature mirror-glaze wax (Meguiar's, Inc., Irvine, CA) was used as the mold-releasing agent.

First, a known amount of epoxy resin (DER 332) was placed in a beaker. Because the epoxy partly crystallized at room temperature, it was heated at 80°C for half an hour so that the epoxy crystals melted and the absorbed moisture was removed. To this, a stoichiometric amount of amines was added and mixed thoroughly. The prepared mixture was then cast in the aluminum mold. Then, they were cured and postcured at different temperatures to obtain full conversion of the epoxy. Cured samples of stoichiometrically mixed amines and epoxy were prepared with different mixing ratios and cure schedules. For all formulations containing different mixing ratios, curing was done initially at 80°C for 3 h and at 100°C for 1 h, and then postcuring was performed. Table I shows the different stoichiometric mixing ratios and postcuring temperatures. Preliminary measurements showed that too high a postcure temperature for the lower functionality resins resulted in the undesired etherification reaction shown in Figure 2(c). Therefore, those mixtures were postcured at 100°C.

Viscoelastic measurement

A TA Instruments (Ettenleur, Netherlands) model Q800 dynamic mechanical analyzer was used. A viscoelastic study of the cured resins was done on rectangular bars of cured specimens in the tension mode at different frequency sweeps (0.3–60 Hz) at a heating rate of 1°C/min. The evolution of the storage modulus (E') and energy dissipation (tan δ) with the temperature was measured. The resulting viscoelastic data were then shifted along the frequency axis to obtain both a master curve and the corresponding shift factor curve.

Differential scanning calorimetry (DSC)

A TA Instruments DSC2920 differential scanning calorimeter was used to measure the reaction heat of the epoxy cured with different stoichiometric ratios of amines. The heating rate was 10°C/min from −50°C to an ending temperature of 175°C under a nitrogen atmosphere.

Density

The densities of the cured resins were measured with Archimedes' principle, which states that the volume is proportional to the difference in the weight between dry and submerged samples. The experimental setup consisted of a weighing balance and glass filled with silicone oil (type M100, Dow Corning, Haltermann B.A.B.V., Kallo, Belgium).

Crosslink density calculation

To relate the resin chemistry to the viscoelastic behavior, the crosslink density has to be determined. ν_c^{calc}, which is a function of the conversion (p_A), mixing ratio (r_A), and functionality (f_i), can be determined from the Miller–Macosko theory[2,3] and is given by the following relation:

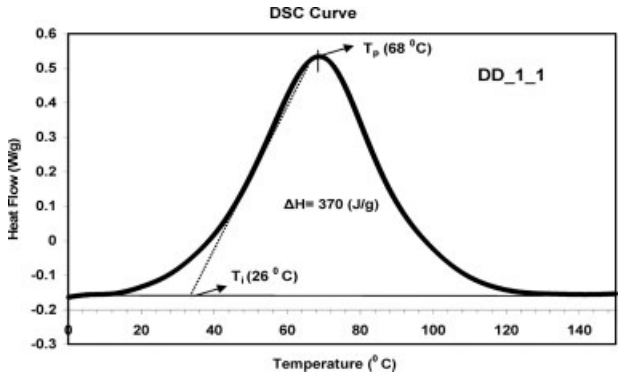

Figure 3 Cure initiation temperature (T_i), peak curing temperature (T_p), and reaction enthalpy (ΔH) of DD_1_1 in DSC. T_i is the point of intersection of the dotted line and the baseline line. T_p is the temperature at the maximum heat flow (W/g). ΔH is the total area under the peak curve and baseline.

$$\nu_c^{calc} = \frac{\sum_{m=3}^{f_k} \frac{m-2}{2} \sum_{f_i=m}^{f_k} n_{Ai0} P_{m,f_i}(x)}{V} \tag{5}$$

where n_{Ai0} is the molar concentration of A_f, f_k is the highest functionality, and V is the network volume related to the mass network (M_n). The density (ρ) is determined as follows[2]:

$$V = \frac{M_n}{\rho} \tag{6}$$

$P_{m,fi}(x)$ is the probability that an A_f, monomer has become an effective crosslink of degree m:

$$P_{m,f_i}(x) = \binom{f_i}{m} x^{f_i - m}(1-x)^m \tag{7}$$

x stands for the probability that a randomly picked A_f group is connected to a finite chain (dangling end). This quantity follows by solving

$$p_A \sum b_j \left[1 - r_A p_A \left(1 - \sum a_i x^{f_i - 1}\right)\right]^{g_j - 1} - x - p_A + 1 = 0 \tag{8}$$

where $0 < x < 1$. A numerical solution for x is readily obtained with mathematical tools such as MatLab. For the system $A_2 + A_3 + A_4 + B_2$, however, a closed-form solution exists:

$$x = \frac{\sqrt{a_3^2 - a_4\left(3a_4 + 2a_3 + 4a_2 - \frac{4}{r_A p_A}\right)} - a_3}{2a_4} - \frac{1}{2} \tag{9}$$

RESULTS AND DISCUSSION

DSC studies

DSC was used to find the cure initiation temperature, peak curing temperature, and enthalpy during the reaction, as shown in Figure 3. Table II shows the DSC results. The DSC data show that in all the epoxy–amine mixtures, there was a single exothermic reaction peak. The cure initiation temperature[4,5] increased from 26 to 56°C from the two-functional amine to the four-functional amine in the epoxy–amine mixture. This was expected because the two methyl substituent groups in the two-functional amine curing agent (DMEDA) act as electron-activating groups and increase the reactivity of the amine and thereby decrease the cure initiation temperature. In the four-functional amine (EDA), the absence of methyl substituents led to a higher cure initiation temperature. The enthalpy (heat content) increased, with the highest enthalpies for DEM_1_05_05 and DMD_1_05_05 (these mixtures had higher enthalpy than the others). This can be attributed to steric hindrances caused by reactive amine groups during the curing reaction.

Density study

The densities of the cured resins were determined by Archimedes' principle at room temperature. The sample weight was determined in both air and oil. The density was calculated as follows:

$$\text{Density} = \frac{\rho_{\text{oil}} \times \text{Sample}_{\text{dry}}}{\text{Sample}_{\text{dry}} - \text{Sample}_{\text{wet}}} \tag{10}$$

where ρ_{oil} is the density of silicone oil (0.96 g/cm^3), $\text{Sample}_{\text{dry}}$ is the weight of the sample in air (g), and $\text{Sample}_{\text{wet}}$ is the weight of the sample in silicone oil (g). The test procedure was calibrated with polystyrene and polycarbonate samples of known density. An increase in the density was observed from samples containing two-functional amines to four-functional amine epoxy mixtures. This was due to an increase in the network crosslink density. The density values are shown in Table II.

TABLE II
Average Functionality (f), Cure Initiation Temperature (T_i), Peak Curing Temperature (T_p), Reaction Enthalpy (ΔH), and Density Values at Different Stoichiometric Ratios

Sample	f	T_i	T_p	ΔH (J/g)	Density (g/cm^3)
DD_1_1	2.0	26	68	370	1.160
DMD_1_03_07	2.2	28	70	369	1.159
DMD_1_05_05	2.4	33	74	452	1.171
DMD_1_07_03	2.6	28	72	333	1.176
DM_1_1	3.0	39	80	312	1.191
DEM_1_03_07	3.2	47	87	422	1.189
DEM_1_05_05	3.4	40	77	475	1.193
DEM_1_07_03	3.6	51	86	445	1.194
DE_1_1	4.0	56	92	341	1.196

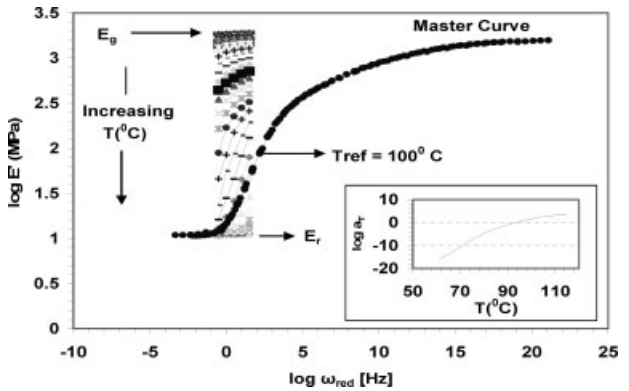

Figure 4 Plot of E' with respect to ω_{red} for the DD_1_1_100_4h formulation. The dotted lines are the modulus values of all frequencies at different temperatures. The master curve is shown by the solid line. A plot of log a_T versus the temperature is shown as an insert.

DMA studies

DMA was used to study the viscoelastic behavior of the thermoset materials. The obtained modulus data at different temperatures from the DMA experiment are plotted with respect to the frequency scale in Figure 4. According to the time–temperature superposition principle,[6] the modulus data can be shifted along the frequency axis to generate a so-called master curve (included in Fig. 4). Figure 4 shows the E' master curve plotted against the reduced angular frequency (ω_{red}) for the DD_1_1 formulation obtained after the shifting of the modulus data on frequency to a reference temperature (T_{ref}) of 100°C.[7] ω_{red} is given by

$$\omega_{red} = \frac{\omega}{a_T} \tag{11}$$

where ω is the angular frequency (rad/s) and a_T is the shift factor. The corresponding shift factor is shown as an insert in Figure 4. If the same shift factor is applied to the loss modulus (E'') and damping (tan δ) data, the master curves obtained are as shown in Figure 5. This results in a reasonable superposition of this dataset as well. Figure 4 shows the unique E' master curve; therefore, for all our resin formulations, we chose E' data, and their corresponding master curves were obtained. The E' master curves and their corresponding shift factor curves for all our formulations were obtained by the shifting of modulus data toward T_{ref} = 100°C, and they are shown in Figure 6. Figure 6 shows that the rubbery modulus plateau increased steadily from 11 to 34 MPa with the increase in the average functionality. This was due to the increase in the crosslink density of the network formed. We can also see that the viscoelastic-transition region shifted to lower frequency scales with the increase in the average functionality. Note that the glass transition shifted from about 10^{-6} for the curve of an average functionality of 2 to 10^{6} for the curve of an average functionality of 4. This means that there was a shift of 12 decades along the frequency axis. Also in Figure 7, we can see that the log a_T curves shifted to higher temperatures with an increase in the average functionality.

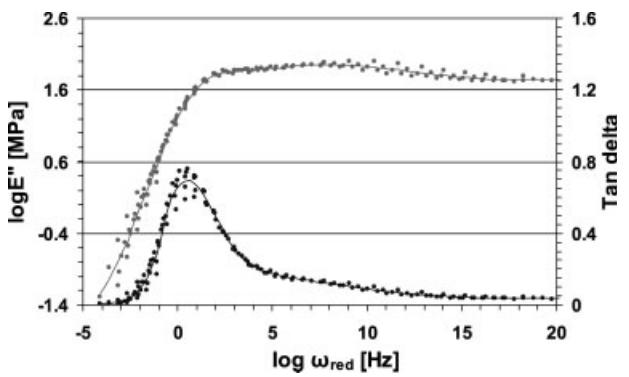

Figure 5 Plot of E'' and tan Δ with respect to ω_{red}. The master curve is shown by dots, and the full line is the average of the dotted points for the DD_1_1_100_4h formulation. The primary axis is for E'', and the secondary axis is for the tan Δ data.

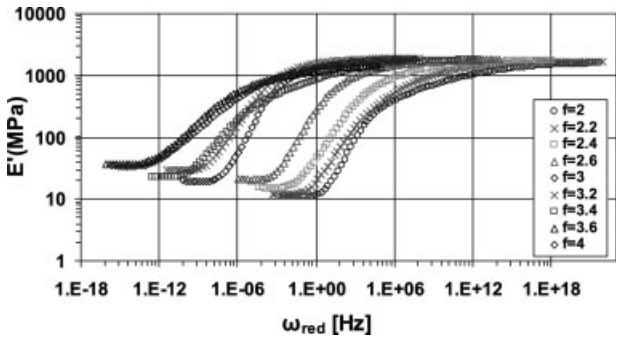

Figure 6 Plot of master curves obtained after frequency–temperature superposition to T_{ref} = 100°C for various average functionality (f) values with respect to ω_{red}.

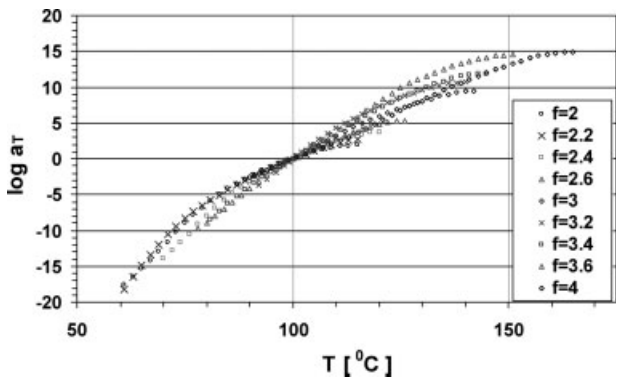

Figure 7 Graph showing a_T values corresponding to the obtained master curves of various average functionality (f) values with respect to the temperature (T_{ref} = 100°C).

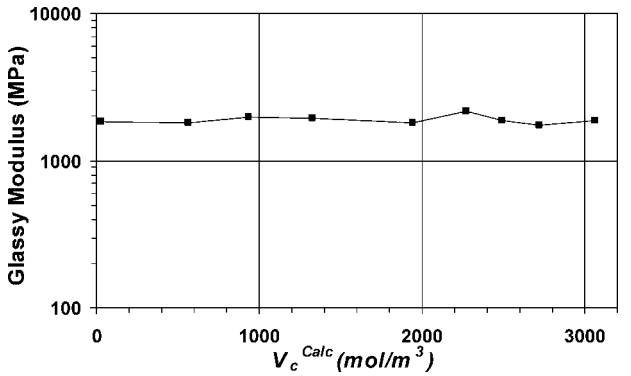

Figure 8 Effect of ν_c^{calc} (mol/m^3) on E_g at 60°C below T_g.

Furthermore, it can be observed from Figure 6 that E_g was not much affected by the functionality of the mixture. This is shown in detail in Figure 8.

In Figure 8, it can be seen that E_g is independent of the crosslink density. This is because below the glass-transition temperature (T_g), the molecular motion is limited, and hence the crosslink density has no effect. A typical viscoelastic master curve (Fig. 4) contains three regions, that is, a glassy plateau, a rubbery plateau, and a transition region. E_g will be seen at a lower temperature (a temperature below T_g). Above T_g, E_r is directly related to the crosslink density. According to the theory of rubber elasticity, E_r is directly proportional to the crosslink density[8]:

$$E_r = 3A\nu_c^{meas}RT \tag{12}$$

where A is the front factor and is often assumed to be unity, R is the Universal Gas Constant and is equal to 8.314 J/mol/K, T is the absolute temperature (K), and ν_c^{meas} is the measured crosslink density. Because some of the viscoelastic data of our DMA studies showed a broad transition region, the minimum E_r value was taken to measure the crosslink density. This is ν_c^{meas}. To compare the ν_c^{meas} and ν_c^{calc} results, a graph (Fig. 9) has been plotted between

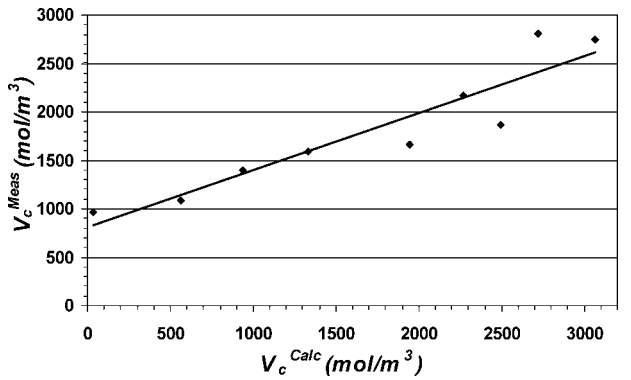

Figure 9 ν_c^{calc} (mol/m^3) versus ν_c^{meas} (mol/m^3) for different stoichiometric formulations.

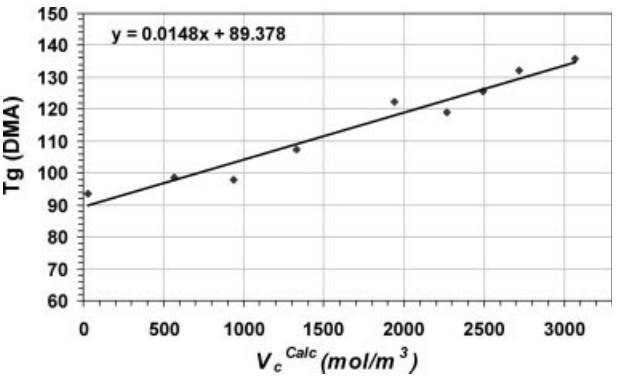

Figure 10 ν_c^{calc} (mol/m^3) versus T_g determined by DMA (T_g is the temperature at the maximum value of tan δ at a frequency of 1 Hz).

ν_c^{calc} (mol/m^3) and ν_c^{meas} (mol/m^3). From Figure 9, it can be seen that ν_c^{calc} agreed relatively well with the ν_c^{meas} values.

The DMA results were also used to determine T_g. T_g is the temperature at which the 1-Hz frequency tan δ curve shows a maximum.[9] To analyze the effect of ν_c^{calc} (determined by the Miller–Macosko theory) on T_g, ν_c^{calc} has been plotted against T_g and is shown in Figure 10. ν_c^{calc} and ν_c^{meas} can be compared with the theoretical crosslink density of Halary's work.[10] T_g increased linearly with the increase in ν_c^{calc}. Figure 10 shows that T_g increased linearly with an increase in ν_c^{calc} (mol/m^3), and this can be modeled as follows[11]:

$$T_g = T_{g\nu_0} + B\nu_c^{calc} \tag{13}$$

where B is the slope, which is of the order of 0.0148 C m^3/mol.[12] $T_{g\nu 0}$ shows the axis offset value, which represents the glass transition for the uncrosslinked linear polymer chains.

Modeling of the relaxation curves

The main features of all the master curves are fitted to the Havriliak–Negami fitting function[13]:

$$E' = E_r + \frac{E_g - E_r}{[1 + (\omega_{red}\tau_0)^{-m}]^n} \tag{14}$$

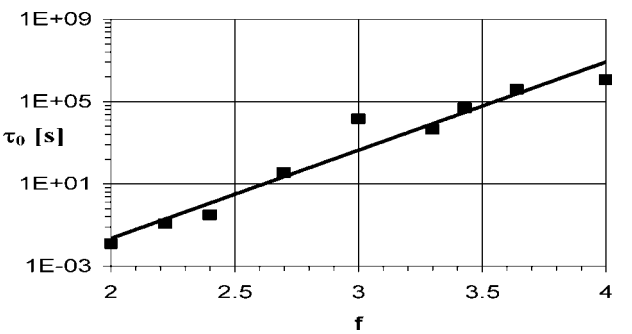

Figure 11 Plot of τ_0 with respect to an increasing average functionality (f).

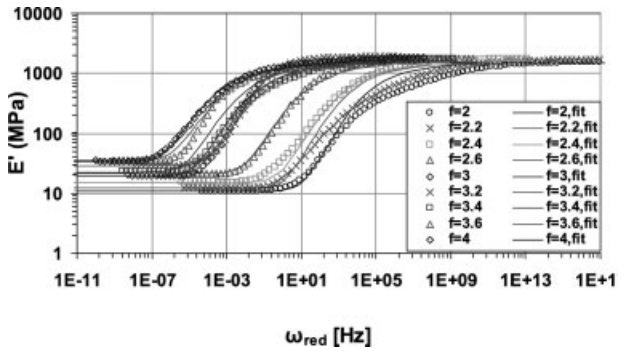

Figure 12 Master curves obtained after the use of a common shift factor in comparison with the globally fitted master curves (full lines; $T_{ref} = 100°C$).

The Havriliak–Negami fitting function is a simple analytical function used to describe the measured relaxation master curves and contains five parameters: E_g (MPa), E_r (MPa), ω_{red} (rad/s), the position of the transition region [i.e., relaxation time constant τ_0 (s^{-1})], and power-law parameters m and n (the shape of the transition region). Parameter m is the slope of the transition region, and n is the slope at the start of the transition. To compare the different experimental master curves, it is necessary to use a common shift factor curve. In our case, this is possible because all experimental curves are already close together. We can therefore choose T_g as T_{ref} and determine the Williams–Landel–Ferry fitting parameters.

$$\log a_T = \frac{C_1^g(T-T_g)}{C_2^g + (T - T_g)} \tag{15}$$

This common shift factor parameters C_1^g and C_2^g have been determined to be 26.01 and 116.97. It is well known that τ_0 in Eq. (14) depends strongly on the temperature. Therefore, for thermorheologically simple materials, this temperature dependence can be taken into account with the so-called shift function, $a_T(T,T_{ref}) = \tau_0(T)/\tau_0(T_{ref})$. τ_0 is determined at $T_{ref} = 100°C$ as follows:

$$\tau_0 = \tau_{0g} a_T\left(T, T_g\left[\nu_c^{calc}\right]\right) \tag{16}$$

The determined τ_0 values have been plotted against the average functionality to determine the effect of the average functionality on τ_0. It can be seen from Figure 11 that τ_0 increased linearly with respect to the average functionality. The full line in Figure 11 is the prediction using eqs. (16) and (15).

The determined common shift factors C_1 and C_2 were used for obtaining new master curves. The new master curves were then fitted to Eq. (14) to obtain a set of single parameters: $E_g = 1500$ MPa, $\tau_{0g} = 1$ s, $m = 0.25$, and $n = 6$. With this set of parameters, global or predicted master curves could be generated for each of the 9 formulations (from an average functionality of 2 to an average functionality of 4). In Figure 12, these predictions (full lines) are compared with the experimental data (symbols). We can see that the Havriliak–Negami fitting function describes the measured curves relatively well.

CONCLUSIONS

In this article, a model is proposed to relate the initial resin chemistry to the viscoelasticity of the final cured product. Bisphenol A epoxy and a series of aliphatic amines were taken as starting reacting compounds and cured and were then tested by DMA for their viscoelastic behavior. It was observed that systematic variation of the functionality and stoichiometry of the reacting compounds led to the shifting of the relaxation master curves by 12 decades on the frequency scale. This was mainly due to the increase in the crosslink density. The measured and predicted crosslink density values were in agreement with each other. The shift of the relaxation master curves to a higher frequency scale, which was due to the increase in the crosslink density, was predicted well. A single set of 9 parameters (m, n, B, ν_c^{calc}, C_1, C_2, E_r, E_g, and τ_0) turned out to be sufficient to describe all viscoelastic data. The deviations of the predicted master curves from the measured curves in some of the cases could be attributed to the difference in ν_c^{calc} and ν_c^{meas}. Finding an optimum cure schedule so that the epoxy is fully reacted with the amine curing agent without any secondary reaction such as etherification (or homopolymerization) is very important in the determination of ν_c^{meas}.

The authors are grateful to Jan de Vreugd and Jos Van Driel for their help in making the aluminum mold.

References

1. Jansen, K. M. B. Bressers, H. J. L; Ernst, L. J. Eng Mater Technol 2006, 128, 478.
2. Macosko, C. W.; Miller, D. R. Macromolecules 1976, 9, 199.
3. Miller, D. R.; Macosko, C. W. Macromolecules 1976, 9, 206.
4. Lobo, H.; Bonilla, J. V. Handbook of Plastic Analysis; Marcel Dekker, Inc: New York, 2003; p 84.
5. Preeti, J.; Veena, C.; Varma, I. R. J Appl Polym Sci 2001, 81, 390.
6. Ferry, J. D. Viscoelastic Properties of Polymers, 3rd ed.; John Wiley & Sons, Inc: New York, 1976; p 271.
7. Plazek, D. J. J Rheol 1996, 40, 987.
8. Hill, L. W. Prog Org Coat 1997, 31, 235.
9. Nielsen, L. E. Mechanical Properties of Polymers and Composites, Marcel Dekker, Inc: New York, 2nd ed.; 1994; p 141.
10. Halary, J. L. High Perform Polym 2000, 12, 141.
11. Fox, T. G.; Flory, P. J. J Appl Phys 1950, 21, 581.
12. Nielsen, L. E. J Macromol Sci Rev Macromol Chem 1969, 3, 69.
13. Szabo, J. P.; Keough, I. A. Thermochim Acta 2002, 392, 1.